Available online at www.sciencedirect.com
ScienceDirect
Ceramics International 35 (2009) 779–786
CERAMICS INTERNATIONAL
www.elsevier.com/locate/ceramint

# Mullite–zirconia–zircon composites: Properties and thermal shock resistance

N. Rendtorff [1], L. Garrido [2], E. Aglietti [3,*]

*Centro de Tecnología de Recursos Minerales y Cerámica (CETMIC; CIC-CONICET-UNLP), Camino Centenario y 506, C.C. 49 (B1897ZCA) M.B. Gonnet, Buenos Aires, Argentina*

Received 14 November 2007; received in revised form 23 November 2007; accepted 19 February 2008
Available online 28 June 2008

**Abstract**

In the refractory field mullite and zirconia are the basis of materials used in the glass industry or when high chemical stability and corrosion resistance are necessary. In this work various mullite–zirconia/zircon compositions were investigated to improve the thermal shock (TS) resistance of dense composites produced by slip casting and sintering at 1600 °C. Zircon ($SiZrO_4$) acts as bonding phase and its thermal decomposition adds zirconia and silica to the material. Resultant composites were characterized by density and dilatometric measurements, XRD and SEM techniques. TS behavior was tested by quenching in water with quenching temperature differentials $\Delta T$ from 400 to 1200 °C. The degree of damage after the TS was experimentally evaluated through the variation of the elastic modulus $E$ which is measured by the excitation technique. The severity of the TS test and the effect of the number of thermal cycles on $E$ for each $\Delta T$ employed were determined.

The tested materials retained their original mechanical properties for temperatures below a critical temperature $\Delta T_c$ near 600 °C. Materials quenched from $\Delta T$ of 1000 °C showed as much as 30% reduction in $E$ indicating the important microstructure damage. The TS resistance improved with increasing zircon addition to 35 wt% in agreement with the behavior predicted from $R$ parameter for crack initiation.


*Keywords:* C. Thermal shock resistance; Mullite–zirconia; Zircon; Elastic modulus

## 1. Introduction

The extensive use of mullite–zirconia (MZ) composites is due to the fact that the zirconia dispersion in the mullite matrix improves the thermo-mechanical properties, leading to toughness by transformation and microcracking. Besides, microcracks originate by the martensitic transformation may cause the dissipation or absorption of potential energy of elasticity by some spreading crack. For this reason these composites are likely to have a good TS resistance [1].

Particularly in refractories, mullite and zirconia are both phases resulting from the use of zircon in high alumina content compositions. Such refractories containing MZ as main phases can be prepared by several routes including sintering electrofused MZ grains which are nowadays available in the market [2–9]. There are also various studies on semi-colloidal and infiltration processing routes [10].

An efficient sintering process of MZ required the use of fine-sized powder and a bonding aid (alumina, zircon, or others) since the electrofused grains are not easy to sintered of their own [6].

Although the thermal shock (TS) can be tested by heating or cooling, it is generally performed by cooling as it provides a severe condition. The method consists in heating samples at high temperature and then quickly cooling them by immersion in water at room temperature (quenching method). Finally, some property is determined before and after the TS experiment such as fracture strength, the Elastic modulus $E$, etc. as these properties are associated with the material microstructure integrity. Thus it is possible to examine the effect of the severity of the thermal cycle and also to correlate the damage evolution after repeated cycles.

* Corresponding author: Tel.: +54 221 484 0247; fax: +54 221 471 0075.
*E-mail address:* eaglietti@cetmic.unlp.edu.ar (E. Aglietti).
[1] Address: CIC, Facultad de Ciencias Exactas-UNLP, Argentina.
[2] Address: CONICET, Argentina.
[3] Address: CONICET, Facultad de Ciencias Exactas-UNLP, Argentina.

0272-8842/$34.00 
doi:10.1016/j.ceramint.2008.02.015

## 2. Experimental

In this study the influence of zircon content, acting as a bonding phase, on sintering properties and the TS behavior of dense MZ–zircon composites was analyzed. The composites containing variable amounts of finer zircon and MZ grains were prepared as bar shape by slip casting in plaster molds. The TS resistance of materials was experimentally followed by measuring $E$, using a dynamic method (impulse excitation technique) [11].

### 2.1. Materials

As a raw material a commercial powder of MZ (MUZR, ELFUSA LT, Brazil) elaborated from the fusion of raw materials of high purity in electrical arc furnaces was used. Table 1 shows the chemical analysis of this electrofused material given by the manufacturer (www.elfusa.com.br). Fusion point: 1850 °C; apparent specific mass (NBR8592-1995): 3.71 g/cm$^3$; apparent porosity (NBR8592-1995): 3.0%; real density: 3.74 g/cm$^3$; reversible linear expansion (1400 °C): 0.68%. The <10 μm fraction (obtained by sedimentation) was milled by attrition up to have a fine powder ($d_{50}$ = 5 μm). This material is composed of mullite and m-$ZrO_2$ as major crystalline phases.

Pure zirconium (Z) silicate (Mahlwerke Kreutz, Mikron, Germany), with a $d_{50}$ of 2 μm, was used as a second raw material.

MZZ composites were prepared from MZ grains and zircon mixtures containing 15, 25, 35 and 45% (in weight basis) of zircon and were called MZZ15, MZZ25, MZZ35 and MZZ45, respectively.

Slip cast compacts consisted of prismatic bars of 4 mm × 3 mm × 45 mm. Concentrated 80 wt% suspensions at pH 9.1–9.2 were prepared by adding the powder to aqueous solutions with 0.3% of dispersant (Dolapix CE64, Zschimmers and Schwartz) and $NH_4OH$. Probes were sintered at a heating rate of 5 °C/min up to different temperatures between 1300 and 1600 °C for 2 h and then cooled to room temperature at 5 °C/min.

### 2.2. Characterization techniques

After drying at 110 °C, density of green bars was determined by mercury immersion. Density and open porosity of sintered samples were determined by the water absorption method. Theoretical density was calculated taking into account the density of each component: 3.16 g/cm$^3$ for mullite, 5.89 g/cm$^3$ for zirconia and 4.56 g/cm$^3$ for zircon.

Crystalline phases formed were analyzed by XRD (Philips 3020 equipment with Cu Kα radiation in Ni filter at 40 kV to 20 mA).

Rietveld method [12,13], a quantitative analysis, was carried out to evaluate the present crystalline phases in the materials. The powder XRD patterns were analyzed with the program FullProf, which is a multipurpose profile-fitting program, including Rietveld refinement [14]. The starting crystallographic data for each phase were extracted from the literature.

The dynamic modulus of elasticity $E$ of composites was measured by the excitation technique with a GrindoSonic, MK5 "Industrial" Model.

For the TS experiments, a water quenching method was used. Thermal cycles with quenching temperature differentials, $\Delta T$ of 400, 600, 800, 1000 and 1200 °C were applied. Sintered sample was heated at a selected temperature in an electrical furnace in air atmosphere for a period of 90 min and then cooled in a water bath at 25 °C. After quenching, samples were dried at 100 °C and then the TS severity effect on $E$ as well as its variation with the number of applied thermal cycles was determined for each $\Delta T$.

Theoretical value of the elastic modulus of the composite materials was evaluated as an average in series using the volume fraction of the existent phases according to the composition determined by XRD, and assuming that the $E$ value of the mullite solid solution is the same as that of the mullite. To calculate the elastic modulus the following Young's modules at zero porosity were used (in GPa): 210 for mullite, 200 for the monoclinic zirconia, and 190 for the zircon [15,16].

Dilatometry of samples sintered at 1600 °C was performed using a Netzsch dilatometer up to 1400 °C at a heating rate of 10 °C/min. The thermal expansion coefficient $\alpha$ up to 1000 °C of these materials was determined.

Microstructural examination was conducted with a scanning electron microscope SEM (Jeol JSM 6360 LV) after polishing the probes surface up to 1 μm diameter diamond paste.

Flexural strength ($\sigma_f$) was measured on bars of rectangular section using a three-point bending tests (Universal testing machine J.J. Instruments) with a 40 mm span and a displacement rate of 2.5 mm/min.

The classical parameter $R$ of the TS behavior was evaluated from $\sigma_f$, experimental $E_0$, $\alpha$ and assuming the same Poisson coefficient $\nu$ for the composites.

Table 1
Chemical composition of the mullite–zirconia (MZ) used www.elfusa.com.br

| Oxide | wt% |
|---|---|
| $Al_2O_3$ | 44.02 |
| $TiO_2$ | 0.29 |
| $SiO_2$ | 17.96 |
| $Fe_2O_3$ | 0.11 |
| MgO | 0.09 |
| CaO | 0.18 |
| $Na_2O$ | 0.16 |
| $K_2O$ | 0.04 |
| $ZrO_2$ | 39.13 |

## 3. Results and discussion

### 3.1. Sintering study

The variation of density and open porosity as a function of sintering temperatures for the different compositions is shown in Fig. 1. Density after a thermal treatment of 1300 °C was slightly higher than the respective green density whereas composites sintered at 1600 °C achieved up to 3.7 g/cm$^3$ in

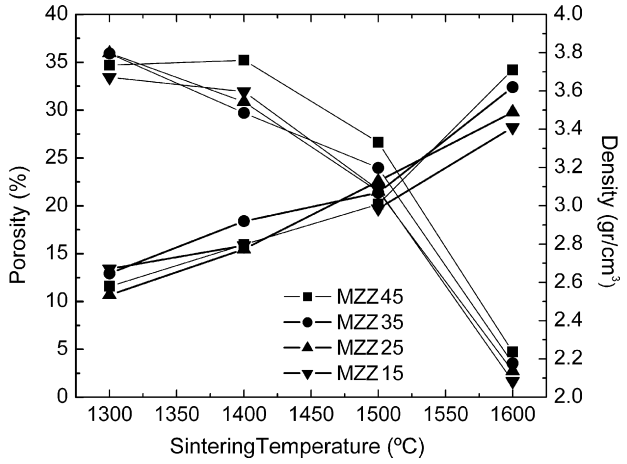


Fig. 1. Porosity and density of materials vs. sintering temperatures.

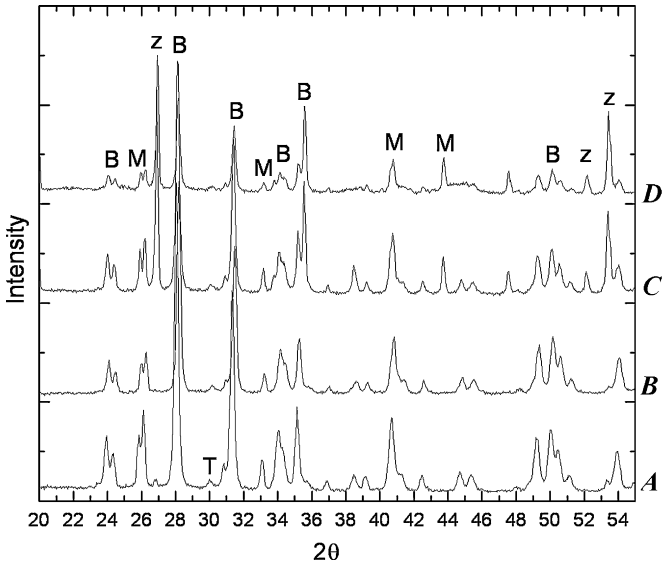


Fig. 2. XRD patterns of sintered composites: MZZ15 (A), MZZ25 (B), MZZ35 (C) and MZZ45 (D) where B, M, z, T corresponds to m-$ZrO_2$, mullite, zircon and t-$ZrO_2$, respectively.

concordance with a marked decrease in porosity. Density was smaller than the theoretical ones which ranged between 4.2 and 4.3 g/cm$^3$. Therefore, to obtain dense materials from these mixtures it was necessary to reach the highest temperature (1600 °C).

Table 2 shows the physical characteristics of the samples sintered at 1600 °C for 2 h.

All samples had similar density and open porosity (lower than 6%) and low water absorption. Density of the sintered materials increased linearly with the zircon content due to the high amount of unreacted zircon and zirconia which are the phases of high density.

Diffractograms of the materials sintered at 1600 °C are shown in Fig. 2. The composites MZZ15 and MZZ25 show that mullite and m-$ZrO_2$ are the crystalline phases present. Besides, there is no zircon reflections appeared in the DRX patterns at $2\theta = 26.98^\circ$ and $53.48^\circ$ showing that maximum decomposition of zircon occurred after treatment at 1600 °C. On the contrary, for MZZ35 and MZZ45, peaks of zirconium silicate were clearly evidenced, which had a high intensity in MZZ45. In both cases, the main phases were zirconia, mullite and zircon. It was found that for MZZ15 about 5% of total zirconia was as t-$ZrO_2$, this phase was not present in the milled MZ starting material [6].

Fig. 3 shows the variation of the crystalline phase contents for the different starting compositions. Crystalline mullite, zirconia and zircon were calculated by the Rietveld method.

A change in composition after sintering at 1600 °C was determined. The added zircon partially or completely dissociated into zirconia and silica. Pure zircon decomposition is reversible; however, impurities, other phases and the cooling rate used make possible that $ZrO_2$ remained at room temperature. Therefore, zirconia content increased due to zircon decomposition reaching 53 and 55 wt% for MZZ15 and MZZ25, respectively, whereas a slight increase to a lower value of 44 and 38 wt% for MZZ35 and MZZ45, respectively, samples was found.

The final composites MZZ35 and MZZ45 contained 20 and 30 wt% of zircon. Therefore the amount of dissociated zircon remained nearly constant (15–20 wt%) and was independent on the initial composition. Mullite content gradually reduced as the relative proportion of the other constituents increased.

Silica can appear in three different ways which include a crystalline form (cristobalite or tridymite), an amorphous phase or a solid solution with mullite. However, in our samples, it was not possible to distinguish the silica phases formed from the zircon decomposition. The main thermal treatment was not long enough to allow $ZrO_2$ forming a solid solution with mullite [17]. So zircon decomposition forming a non-crystalline phase occurred in the four samples due to the thermal treatments conditions. We estimate in 15–20 wt% the amount of the rich silica non-crystalline phase in the materials coming from the zircon decomposition. This fact was proven when the samples where submitted to an annealing thermal treatment at 1500 °C during 15 h. After the annealing the amount of crystalline zircon was increased in the materials. The silica rich non-crystalline phase is dependent on the cooling rate.

Table 2
Physical and mechanical properties of the material sintered at 1600 °C for 2 h

| | Green density (g/cm$^3$) | Apparent density (g/cm$^3$) | Open porosity (%) | Water absorption (%) | $\sigma_f$ (MPa) | $R$ (°C) |
|---|---|---|---|---|---|---|
| MZZ15 | 2.4 | 3.45 | 3.7 | ∼1 | 100 | 95 |
| MZZ25 | 2.4 | 3.50 | 4.3 | ∼1 | 140 | 130 |
| MZZ35 | 2.5 | 3.60 | 3.6 | ∼1 | 150 | 130 |
| MZZ45 | 2.5 | 3.65 | 5.6 | 2 | 170 | 140 |

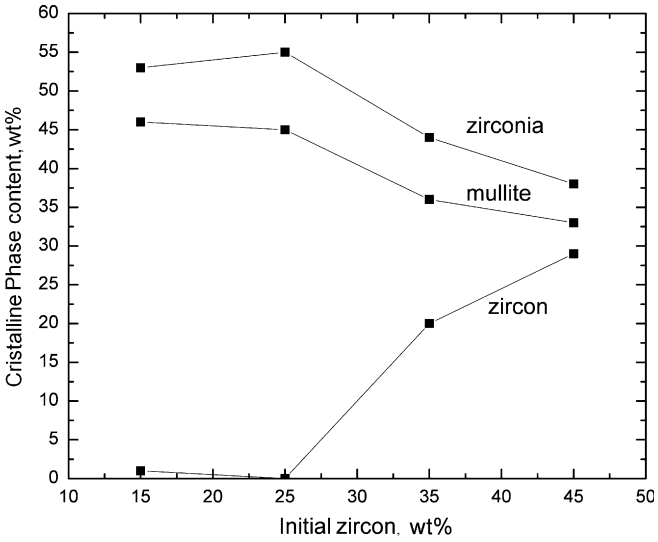


Fig. 3. Crystalline phase contents calculated by the Rietveld method vs. initial amount of zircon.

### 3.2. Microstructure

SEM micrographs of the four materials are shown in Fig. 4. All the samples had a dense microstructure with low residual pore presence which is similar to that reported in previous works [5,6,20], but some differences existed that possibly can explain the different behavior observed to the TS test. Glassy phase is not detectable in the micrographs.

For MZZ15 and MZZ25 samples in which zircon almost decomposed completely, two types of grains were observed: the uniformly dispersed grains of zirconia (white) and the mullite matrix (gray).

Three types of grains were noticeable with higher zircon contents: (a) a completely dispersed (white) of zirconia, (b) grains of unreacted zircon (middle gray) and (c) mullite matrix (dark gray). Phase identification was carried out by EDAX.

$ZrO_2$ grain size ranged between 1 and 7 μm which were slightly larger than those of starting MZ grains ($d_{50}$ = 5 μm). Some zirconia grains appeared bound forming a well-developed neck between them. This fact indicated that the

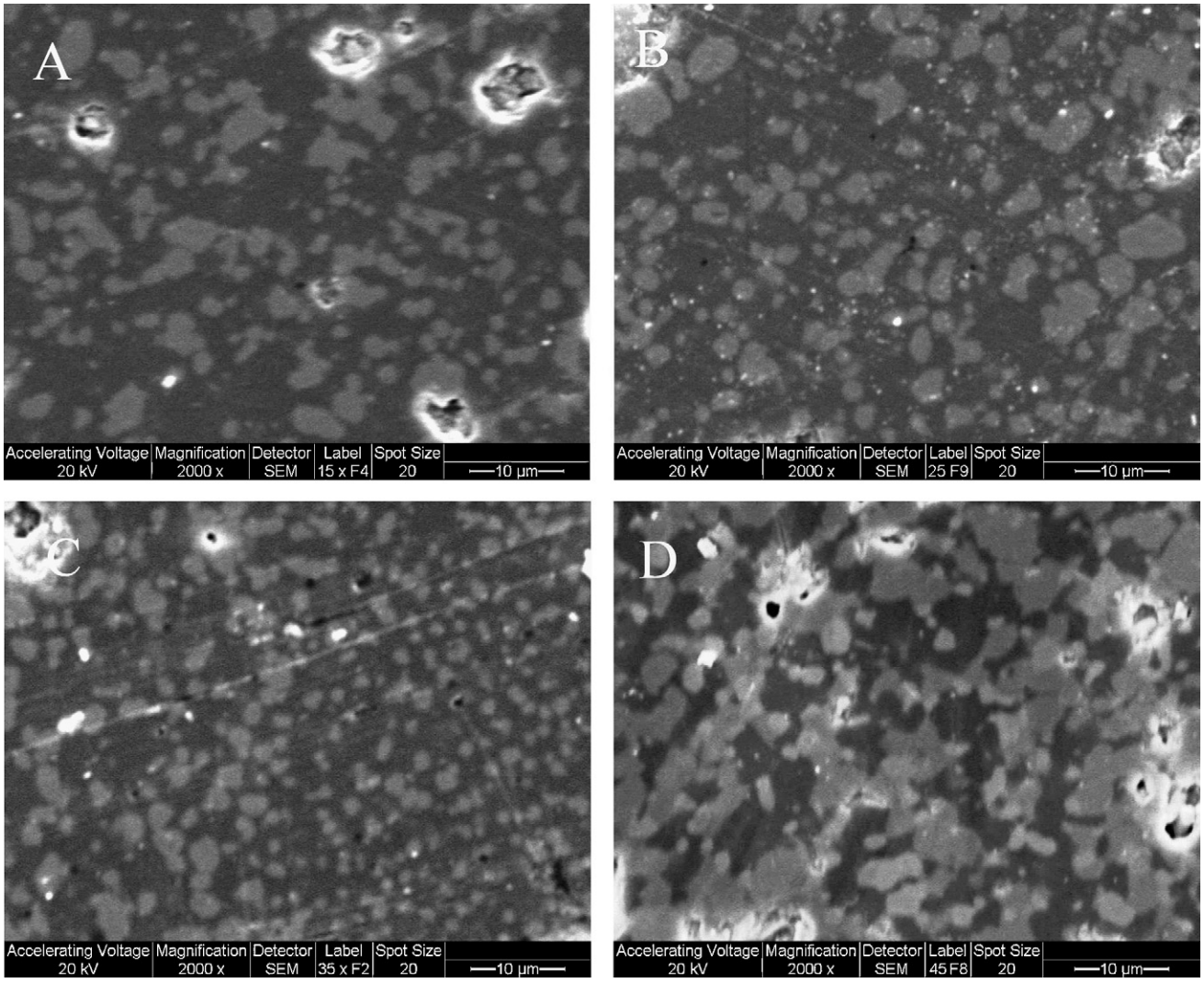


Fig. 4. SEM micrographs of the materials studied: (A) MZZ15, (B) MZZ25, (C) MZZ35 and (D) MZZ45 (bar 10 μm).

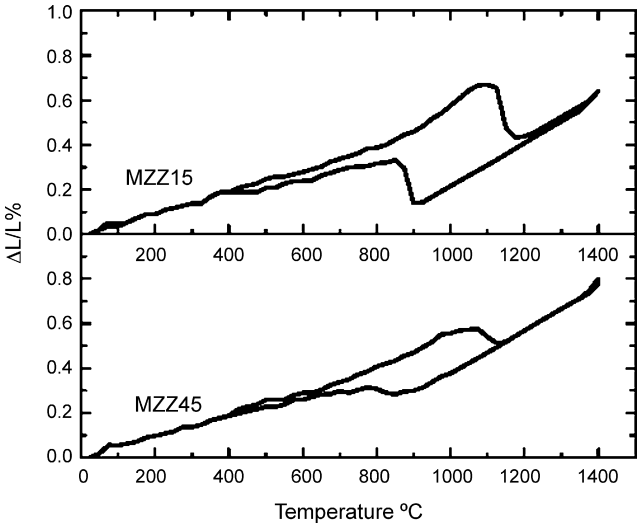


Fig. 5. Dilatometric curves of MZZ15 and MZZ45 materials sintered at 1600 °C.

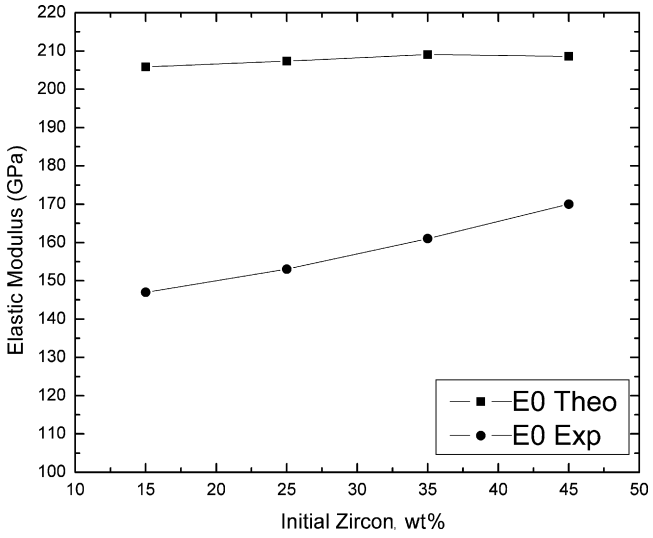


Fig. 6. Theoretical and experimental elastic modulus of the materials.

sintering conditions employed (1600 °C for 2 h) was enough to reach sintering and promoted the zirconia grains growth.

### 3.3. Dilatometry

Dilatometric curves of the MZZ15 and MZZ45 sintered at 1600 °C are shown in Fig. 5. Both curves presented a hysteresis loop area, due to the volume change associated to the m ↔ t-$ZrO_2$ transformation. For MZZ15 this transformation begins around 1100 °C on heating and the extended loop was in accordance with the highest content of m-$ZrO_2$ determined by the Rietveld method (Fig. 3). Contrarily, the relatively small hysteresis loop area for the MZZ45 was due to a low amount of transformable zirconia. Therefore, a low amount of microcracks developed in MZZ45. Thus, the high separation distance between cracks was less favorable for nucleation or linkage of existing cracks.

The thermal expansion coefficient of these materials up to 1000 °C was near $5.0 \times 10^{-6}$ °$C^{-1}$, comparable with that of mullite and zircon (5.3 and $4.2 \times 10^{-6}$ °$C^{-1}$, respectively). Nevertheless, a reduction in the local thermal mismatch with increasing the amount of zircon in the microstructure probably occurred because of the similar thermal expansion coefficient of mullite and zircon.

The composites studied were sintered at 1600 °C, but on cooling the monoclinic phase transformation took place in those grains having a size higher than the critical one, as is seen by XRD. During the TS test, when thermal cycles of $\Delta T = 1000$ and 1200 °C were applied, the m ↔ t phase transition occurred during heating quenching. For $\Delta T = 1200$ °C, the transformation was completed, while it partially proceed for $\Delta T = 1000$ °C and no phase transition occurred for lower $\Delta T$.

### 3.4. Elastic modulus $E_0$ and flexural strength

Fig. 6 shows the experimental and theoretical modulus of elasticity $E_0$ for the different composites.

Experimental $E_0$ of approximately 70–80% of the theoretical $E$ agreed well with those values reported in an earlier work [16]. Porosity, and any other microstructure defect, likes grain boundaries, cracks or microcracks decrease the elastic modulus. Full densification of ceramics was very difficult to obtain. Also, certain defects were originated from volume changes due to m ↔ t-$ZrO_2$ phase transformation during processing. Additionally, any glassy phase lowered the elastic modulus of the composite. Therefore, besides porosity, the low experimental $E_0$ may be explained by the presence of inherent defects due to the processing.

If we consider that porosity was similar for all the materials (Table 2) the increase in $E_0$ value when zircon content increased was probably due to a lower number of microcracks originated from the m ↔ t transition. The amount of microcracks may be related to the loop area of the dilatometric curves (Fig. 5).

The flexural strength $\sigma_f$ (Table 2) showed a gradual increase with the amount of zircon in the original composition. These values are slightly lower than that reported in the literature for pure mullite [18], MZ (about 215 MPa) [19] and pure zircon (150–320 MPa) for various products fabricated at 1600 °C [20]. The difference may be explained by the residual porosity and the formation of microcracks due zirconia transformation during cooling.

### 3.5. Thermal shock behavior

#### 3.5.1. Effect of quenching temperature difference ($\Delta T$) on the $E_1/E_0$ ratio

The TS behavior of composites was evaluated by measuring the decrease in $E_1/E_0$ ratio where $E_0$ and $E_1$ are the original elastic modulus and that after one quenching, respectively. Fig. 7 shows the evolution of $E_1/E_0$ ratio, with $\Delta T$. Fig. 7 indicates that the degree of damage was not significant up to $\Delta T \approx 600$ °C while it get greater when the applied $\Delta T$ increased up to 1000 °C. Thus, the $\Delta T_c$ of the materials was near to 600 °C. The $E_1/E_0$ remained unchanged at low $\Delta T$ whereas a

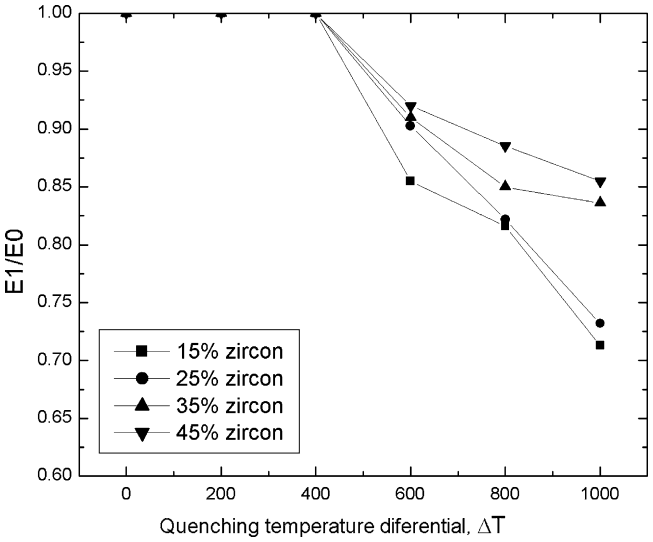


Fig. 7. Effect of quenching temperature differences ($\Delta T$) on the $E_1/E_0$ ratio.

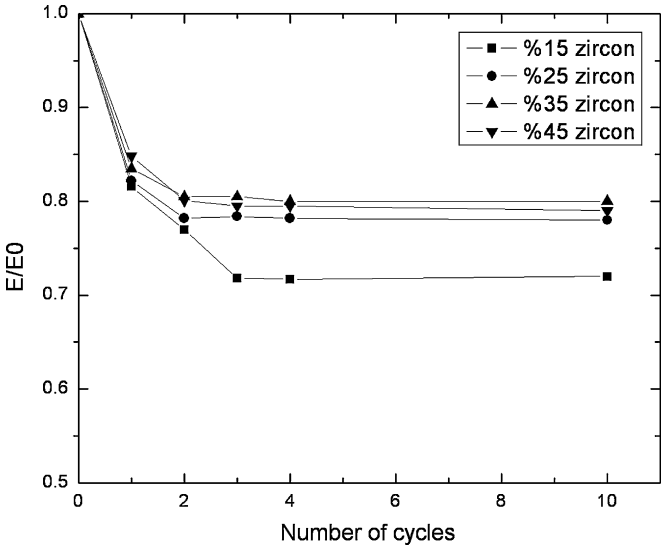


Fig. 8. Evolution of $E/E_0$ ratio with the number of thermal cycles at $\Delta T = 800$ °C applied for the different materials.

reduction of 20–30% was caused by more severe shocks. The decrease in $E_1$ was lower with increasing zircon content. Most of probes dramatically failed under a TS with $\Delta T = 1200$ °C, which did not allow extrapolate the obtained results to the actual operating conditions. This general behavior is well explained and predicted by the classical TS resistance thermoelastic model and Hasselman unified theory [21].

Fig. 7 also shows that probes with greater zircon content exhibited a high $E_1$, it means, and that the microstructure of these quenched probes was less degraded by one TS test probably due to low amount of microcracks present in the material. This behavior was clearly evidenced when a $\Delta T = 1000$ °C was employed, because at this $\Delta T$ the m ↔ t transition took place. Thus, the important microcrack formation due zirconia phase transformation caused a great drop in $E_1$.

Table 3 shows the initial flexural strength for the different compositions. Increasing zircon addition improved flexural strength probably due to the gradual porosity reduction. The parameter $R$ resulted a rather lower relative to a $\Delta T_c$ of 600 °C. However, the high $R$ parameter represented an increase in the TS resistance with addition of zircon.

Consequently, as the experimental $\Delta T_c$ was close to 600 °C, the effect of the number of thermal cycles on the $E/E_0$ ratio was examined for $\Delta T$ of 1000 and 800 °C.

### 3.5.2. *Effect of the number of quenching cycles on the $E/E_0$ ratio for different $\Delta T$*

Fig. 8 shows the evolution of the $E/E_0$ ratio being $E_0$ and $E$ for original and quenched samples, respectively, with the number of quenching cycles at $\Delta T = 800$ °C for the different compositions. The effect on elastic modulus of cracks and microcracks was reviewed by Brand [22] and later by Stiffler and Hasselman [22,23]. There was a rapid $E/E_0$ drop after few cycles, and then a gradual reduction up to achieve a nearly constant value with increasing the number of cycles. This is a typical behavior previously reported in the literature [5,6]. Most composites retained $E$ of about 80% of the $E_0$ indicating an important microstructure degradation. By applying three thermal cycles, the material MZZ15, prepared from the composition with a low amount of zircon, showed the greater degradation indicating that new cracks were formed. However, $E/E_0$ remained constant and close to 0.7 up to 10 cycles proving that no greater crack propagations occurred [18].

The TS behavior using a $\Delta T = 1000$ °C of the different materials is shown in Fig. 9. The $E/E_0$ followed a similar

Table 3
Phase composition of initial MZ and Z mixtures

| | Mullite (wt%) | $ZrO_2$ (wt%) | Zircon (wt%) |
|---|---|---|---|
| MZZ15 | 47 | 38 | 15 |
| MZZ25 | 41 | 34 | 25 |
| MZZ35 | 36 | 29 | 35 |
| MZZ45 | 30 | 25 | 45 |

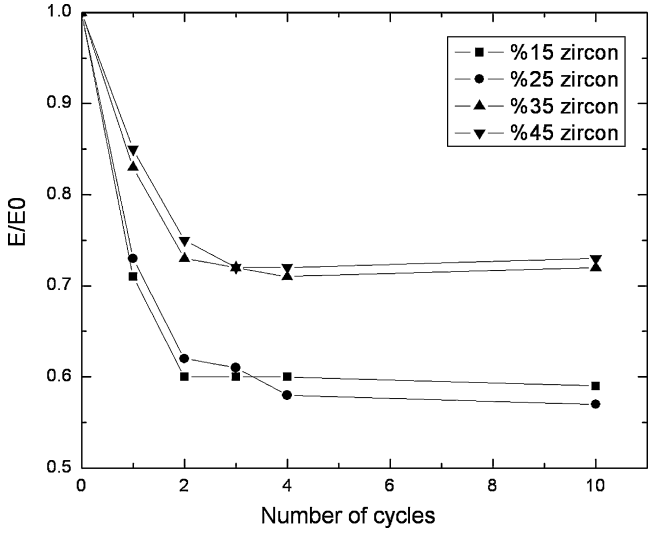


Fig. 9. Evolution of $E/E_0$ ratio with the number of thermal cycles at $\Delta T = 1000$ °C applied for the different materials.

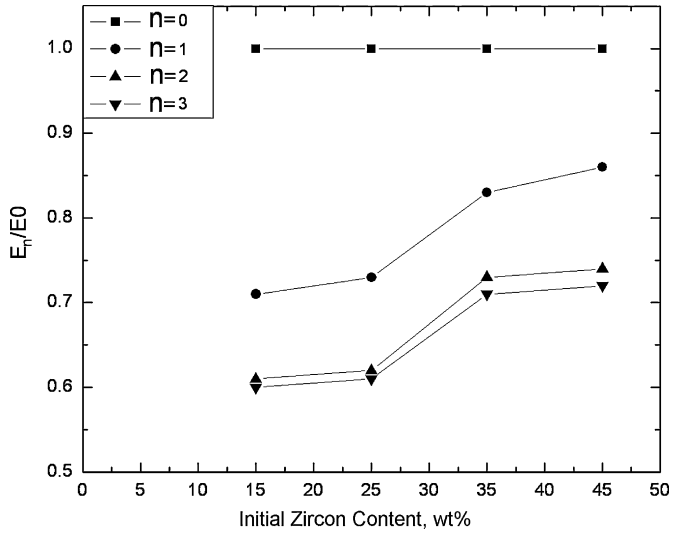


Fig. 10. Evolution of the $E_n/E_0$ ratio with zircon addition for various numbers ($n$) of thermal cycles at $\Delta T = 1000\ ^\circ C$.

behavior with the number of cycles applied than that observed in tests with $\Delta T = 800\ ^\circ C$. For MZZ15 and MZZ25, the reduction of $E/E_0$ was similar and close to 40% after the two first cycles. Contrarily, the compositions with 35 and 45% of zircon showed a better TS behavior as for both cases the residual $E$ was more than 70% of the original.

Fig. 10 shows the evolution of the $E/E_0$ ratio with zircon addition for various numbers of thermal cycles when a $\Delta T = 1000\ ^\circ C$ was applied. There was observed a sudden change in the TS behavior when the zircon percentage varied from 25 to 35%. This change was related to the low content of zirconia as well as the presence of the unreacted zircon as a disperse phase (see Fig. 3 and SEM micrographs in Fig. 4).

The influence of zircon content on high alumina–mullite refractories was studied by others authors [10,24–27]. Zircon improved the TS resistance and gave a higher resistance to fracture damage, so a long-life performance on service results. As was reported a 20 wt% of zircon content enhanced some properties such as lowered the porosity, improved the interparticle bond and also caused a microstructural toughening due to the zirconia content. We have found that a dense ceramics produced from a 35 wt% addition of zircon containing higher zirconia proportion but no alumina resulted in a higher TS resistant material.

## 4. Summary and conclusions

MZ–zircon composites containing up to 30 wt% of zircon ($ZrSiO_4$) were produced by slip casting and heating at 1600 °C. Their TS resistance was determined by quenching in water and satisfactorily predicted using the $R$ parameter.

Density as well as flexural strength and the elastic modulus of starting composites slightly increased with zircon in the mixture. For 35–45 wt% zircon content, zircon partially dissociated under thermal treatment and remained like a dispersed phase whereas in materials with lower additions the decomposition was complete.

TSs of $\Delta T = 600\ ^\circ C$, produced a significant decrease in the elastic modulus, which was more important as $\Delta T$ increased due to the development of internal microcracks, propagation of preexistent cracking and new cracking formation. This critical temperature, known as $\Delta T_c$, slightly changed with zircon addition. For $\Delta T = 1000\ ^\circ C$ more severe microstructure degradation occurred due to the zirconia m ↔ t transition.

At $\Delta T$ 800–1000 °C, $E/E_0$ followed a well-defined exponential decay behavior with increasing number of cycles. After three cycles, $E/E_0$ reduced to a nearly constant value proving the good resistance to cracking propagation and growth.

TS resistance markedly improved in composites having 20–30 wt% of zircon. The high TS resistance may be explained by several factors such as: a relative low amount of transformable m-$ZrO_2$ grains which, in turn, controlled the amount of the microcracks and a local reduction of thermal mismatch. Besides, the parameter $R$ predicted a comparable behavior with the improved TS resistance with zircon addition.

## Acknowledgements

The authors are indebted to S. Conconi for the Rietveld analysis. N. Rendtorff also expresses gratitude to CIC for the scholarship.

## References

[1] H. Zender, H. Leistner, H. Searle, $ZrO_2$ materials for applications in the ceramic industry, Interceramics 39 (6) (1990) 33–36.
[2] P. Descamps, S. Sakaguchi, M. Poorteman, F. Cambier, High temperature characterization of reaction sintered mullite–zirconia composites, J. Am. Ceram. Soc. 10 (1991) 2476–2481.
[3] N. Claussen, J. Jahn, Mechanical properties of sintered in-situ reacted mullite–zirconia composites, J. Am. Ceram. Soc. 3/4 (1980) 228–229 (Note).
[4] K. Das, S.K. Das, B. Mukherjee, G. Barnerjee, Microstructural and mechanical properties of reaction sintered mullite–zirconia composites with magnesia as additive, Interceramics 5 (1998) 304–313.
[5] L.B. Garrido, E.F. Aglietti, Zircon based ceramics by colloidal processing, Ceram. Int. 5 (2001) 491–499.
[6] F. Temoche, L.B. Garrido, E.F. Aglietti, Processing of mullite–zirconia grains for slip cast ceramics, Ceram. Int. 31 (2005) 917–922.
[7] C. Aksel, Mechanical properties and thermal shock behaviour of alumina–mullite–zirconia and alumina–mullite refractory materials by slip casting, Ceram. Int. 29 (2003) 311–316.
[8] C. Aksel, The influence of zircon on the mechanical properties and thermal shock behaviour of slip-cast alumina–mullite refractories, Mater. Lett. 57 (2002) 992–997.
[9] C. Aksel, The microstructural features of an alumina–mullite–zirconia refractory material corroded by molten glass, Ceram. Int. 29 (2003) 305–309.
[10] S. Maitra, A. Rahaman, A. Sarkar, A. Tarafdar, Zirconia–mullite materials prepared from semi-colloidal route derived precursors, Ceram. Int. 32 (2006) 201–206.
[11] ASTM Standard C1171-05 (2005).
[12] D.L. Bish, J.E. Post, Quantitative mineralogical analysis using the Rietveld full-pattern fitting method, Am. Miner. 78 (1993) 932–940.
[13] Rodriguez, Caravajal, FULLPROF, a program for Rietveld refinement and pattern matching analysis, in: Abstracts of the Satellite Meeting on Powder Diffraction of the IUCr, Toulouse, France, (1990), p. p12.
[14] H.M. Rietveld, A profile refinement method for nuclear and magnetic structures, J. Appl. Cryst. 2 (1969) 65–71.

[15] W. Kingery, Factors affecting thermal stress resistance of ceramic materials, J. Am. Ceram. Soc. 38 (1955) 3–15.
[16] M. Hamidouche, N. Bouaouadja, H. Osmani, R. Torrecillias, G. Fantozzi, Thermomechanical behavior of mullite–zirconia composite, J. Eur. Ceram. Soc. 16 (1996) 441–445.
[17] T. Koyama, S. Hayashi, A. Yasumori, K. Okada, M. Schmucker, H. Schineider, Microstructure and mechanical properties of mullite/zirconia composites prepared from alumina and zircon under various firing conditions, J. Eur. Ceram. Soc. 16 (1996) 231–237.
[18] R. Ruh, K.S. Mazdiyasni, M.G. Mendiratta, Mechanical and microstructural characterization of mullite and mullite–SiC whisker and $ZrO_2$, toughened-mullite–SiC whisker composites, J. Am. Ceram. Soc. 71 (1988) 503–512.
[19] S. Lathabai, D.G. Hay, F. Wagner, N. Claussen, Reaction-bonded mullite/zirconia composites, J. Am. Ceram. Soc. 79 (1996) 248–256.
[20] S. Ying, H. Xiaoxian, Y. Dongsheng, Fabrication of hot-pressed zircon ceramics: mechanical properties and microstructure, Ceram. Int. 23 (1997) 457–462.
[21] D.P.H. Hasselman, Unified theory of thermal shock fracture initiation and crack propagation in brittle materials, J. Am. Ceram. Soc. 52 (1969) 600–604.
[22] R.C. Bradt, Problems and Possibilities with Cracks in Ceramics ‘‘Science of Ceramics’’, vol. 11, Gotemborg, Sweden, 1981.
[23] R.C. Stiffler, D.P.H. Hasselman, Shear moduli of composites with elliptical inclusions, J. Am. Ceram. Soc. 66 (1983) C52–53.
[24] N. Rendtorff, F. Temoche, L. Garrido, E. Aglietti, Choque térmico de cerámicos de Mullita–Zirconia, in: V Congreso Binacional CONAMET/SAM, 2005.
[25] C. Aksel, M. Dexet, N. Logen, F. Porte, F. Riley, F. Konieczny, The influence of zircon in a model aluminosilicate glass tank forehearth refractory, J. Eur. Ceram. Soc. 11 (2003) 2083–2088.
[26] C. Aksel, Mechanical properties of alumina–mullite–zircon refractories, Key Eng. Mater. 3 (2004) 1791–1794.
[27] C. Aksel, Thermal shock behavior of alumina–mullite–zircon refractories, Key Eng. Mater. 3 (2004) 1747–1750.